DOI: 10.12700/AIS.2025.002

Explainable MLP-Based Surrogate Model for Predicting Terahertz Metamaterial Absorber Performance

Nesibe Yalçın
Dept. of Computer Engineering
Erciyes University
Kayseri, Türkiye
nesibeyalcin@erciyes.edu.tr

Sibel Ünaldı
Dept. of Electrical and Electronics Engineering
Bilecik Şeyh Edebali University
Bilecik, Türkiye
sibel.unaldi@bilecik.edu.tr

Gaye Ediboglu Bartos
The Institute of Science and Software Technology
Obuda University, Alba Regia Faculty
Székesfehérvár, Hungary
gaye.ediboglu@uni-obuda.hu

***Abstract*—This study presents an explainable surrogate modeling approach for predicting the absorption behavior of broadband THz metamaterial absorbers based on vanadium dioxide (VO_2) by a Multi-Layer Perceptron (MLP) network. The proposed model was trained on an electromagnetic full-wave simulation dataset, which included design parameters and frequency, with the corresponding absorption as output. The MLP-based surrogate model was evaluated using performance metrics such as the coefficient of determination (R^2), Mean Absolute Error (MAE), and Root Mean Squared Error (RMSE). Additionally, explainable artificial intelligence (XAI) methods were used to understand how the input parameters affect the absorption. Thus, the proposed model offers important clues regarding the physical relationship between design parameters and absorption performance. The results obtained indicate that the MLP model achieves high prediction accuracy. This approach offers a promising alternative for the design and optimization of next-generation THz absorber devices.**

***Keywords*—absorption, XAI, metamaterial, MLP, SHAP, surrogate modeling, Terahertz.**

I. Introduction

With the development of wireless communication technologies, especially 6G networks, TeraHertz (THz) frequency components have received attention from researchers owing to their potential for ultra-high data rates of up to 1 Tbps and low latency [1], [2]. Metamaterial absorbers have emerged as crucial components due to their ability to selectively absorb electromagnetic waves, thereby enhancing signal quality and reducing interference [3]. They provide control over wave absorption, which is essential for applications in security, imaging, sensing, and privacy technology, as well as in communications [4] - [6]. Among the various materials used in metamaterial component design, vanadium dioxide (VO2) is notable for its exceptional phase-transition properties [7]. VO2 experiences a reversible metal-insulator transition near room temperature, thus allowing the electromagnetic response of the absorber to be dynamically tuned [8], [9]. Due to their tunability, VO2 based metamaterial absorbers can be good candidates for smart communication systems and adaptable THz devices [10], [11].

However, the use of simulation approaches in the design process can make these absorbers costly and time-consuming. Machine Learning (ML) has become a useful technique for addressing these problems by providing faster and more reliable prediction capabilities. A dataset was introduced in [12] to analyze THz metamaterials and train ML models. A data-driven surrogate-assisted model for the design optimization procedure of a metamaterial-based filtenna using deep learning was presented in [13]. Data-driven approaches in metamaterial design have been highlighted in recent research [14], which shows that ML techniques can be used to effectively predict the bandwidth and gain of metamaterial antennas.

A new strategy is needed to build trust in artificial intelligence and ML models. Despite progress in recent decades, interpretability and black box issues remain pervasive [15]. Due to their “Black Box” structure with limitations on their interpretability, ML models are often criticized [16]. Explainable Artificial Intelligence (XAI) addresses these challenges. Understanding the impact of input parameters on the model's predictions is crucial to ensure interpretability and facilitate effective debugging of the surrogate model [17].

In this work, a Multi-Layer Perceptron (MLP) model integrated with SHapley Additive Descriptions (SHAP), a method from XAI, was used for the interpretable prediction of the absorption performance of a metamaterial absorber. SHAP analysis was used to identify the critical input parameters and their interactions that affected the single output prediction. An MLP model was then developed using this information to improve the prediction performance. The developed model not only makes accurate predictions but also explains their underlying logic, enabling the design of advanced metamaterial absorbers for 6G and other THz applications.

II. Unit Cell and Dataset

The unit cell geometry and design parameters presented in [12] are shown in Fig. 1. The design parameters of the unit cell of the metamaterial absorber are important to achieve the desired electromagnetic response. The unit cell design has a periodicity of (a) 13 µm and a dielectric substrate thickness (h) of 6 µm. The metallic and VO2 layers follow the standard thicknesses defined in [12]. The structure consists of two concentric rings: the outer ring has an outer radius (*Roh*) of 6.5 µm and an inner radius (*Rih*) of 5.5 µm, whereas the inner ring has an outer radius (*Ro2*) of 2 µm and an inner radius (*Ri2*) of 1 µm. The gap between these rings has a width (*w*) of 1 µm.

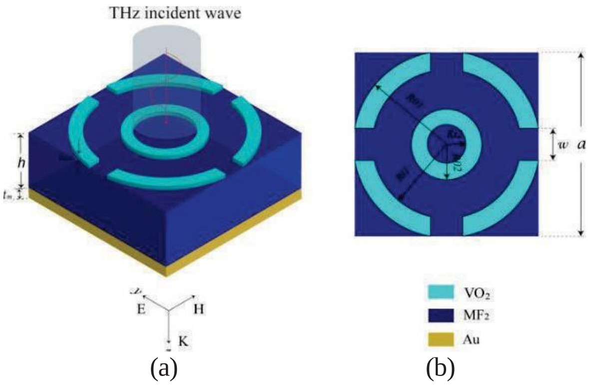

Fig. 1. Schematic of the metamaterial absorber (a) perspective view of the unit cell, and (b) top view [12].

The dataset [18] used in this study was generated through electromagnetic simulations by performing a parameter sweep on the design parameters of a metamaterial absorber's unit cell design, as described in [12]. It is publicly available on Kaggle [18] under the title "Metamaterial Absorber Dataset". The dataset contains three input parameters, as listed in Table I, and an output (absorptance). It comprises a total of 9,018 data points. The presented MLP-based surrogate models were trained on this dataset to predict the absorptance in the operational THz frequency band.

TABLE I. INPUT FEATURES OF THE DATASET [12]

Feature	Symbol	Range	Unit
Patch Width, p	*a*	11 – 14	µm
Dielectric Thickness, m	*h*	3 – 8	µm
Frequency	*f*	0 – 18	THz

III. MLP

Artificial Neural Networks (ANNs) were developed inspired by biological neural networks [19]. MLP is a type of ANNs and consists of fully connected neurons, which communicate with each other in a feedforward manner. MLP networks can perform a wide range of classification and regression prediction tasks with high accuracy or low error. On the other hand, owing to the complex architecture of MLP networks, the internal logic of the network is not understandable or explainable. Black box models are defined as these systems that, when given the correct input, produce the correct output without providing any explanation of how they operate inside [19] - [21].

IV. SHAP

The interpretability or comprehensibility of ML models is as important as their predictive accuracy in several fields [22]. MLP neural networks can deliver superior accuracy predictions but lack interpretability due to their black box nature. Understanding the influence of input features on model decisions is important because it affects overall confidence in model outcomes. Moreover, it is crucial for their applicability, especially in complex or high-risk fields [16].

In this study, SHAP [23] technique was applied to analyze feature contributions and interpret the predictions produced by MLP models. In this technique, all possible feature subsets are comprehensively evaluated, and a contribution/importance value is assigned to each feature [24]. This assigned value, known as the Shapley value, is the average marginal contribution of a feature value for a specific prediction task [25]. Each feature may have a positive or negative impact on model predictions depending on its SHAP value.

V. EXPERIMENTAL STUDIES

In this work, the Python programming language on the Google Colab platform was used to implement MLP network models for predicting the performance of THz metamaterial absorber. Pandas, Matplotlib, Sklearn, TensorFlow, Keras, and Shap open-access libraries were used. The dataset was split into two parts for training and testing at the most common split rate of 70/30. All data were normalized using the StandardScaler() function.

As shown in Table II, six different MLP models were implemented and tested to determine the best possible network architecture (max. 200 epochs). Adam optimizer was chosen to minimize the loss function "MSE" during the training of the models, and early stopping was applied as a practical and efficient approach to prevent overfitting.

TABLE II. MLP NETWORK CONFIGURATIONS

Model	Network Structure
MLP-N1	Dense (64) - Activation = ReLU Dropout (0.2) Dense (32) - Activation = ReLU Dense (1) - Activation = Linear
MLP-N2	Dense (64) - Activation = ReLU Dropout (0.2) Dense (1) - Activation = Linear
MLP-N3	Dense (64) - Activation = ReLU Dense (32) - Activation = ReLU Dense (1) - Activation = Linear
MLP-N4	Dense (32) - Activation = ReLU Dropout (0.2) Dense (1) - Activation = Linear
MLP-N5	Dense (128) - Activation = ReLU Dense (32) - Activation = ReLU Dropout (0.2) Dense (1) - Activation = Linear
MLP-N6	Dense (128) - Activation = ReLU Dense (32) - Activation = ReLU Dense (1) - Activation = Linear

Popular metrics (MSE, RMSE, MAE, and R^2) were utilized to assess these network models' performance. Table III presents the prediction results for the MLP models. All the MLP models performed well despite the small number of features and MLP-N6 achieved better performance.

TABLE III. COMPARATIVE EXPERIMANTAL RESULTS

Model	R^2	MSE	RMSE	MAE
MLP-N1	0.9972	0.0004	0.0201	0.0148
MLP-N2	0.9611	0.005569	0.074627	0.059645
MLP-N3	0.9987	0.000190	0.013767	0.007489
MLP-N4	0.9182	0.011723	0.108273	0.090534
MLP-N5	0.9968	0.000459	0.021433	0.015662
MLP-N6	0.9989	0.000164	0.012809	0.007241

Fig. 2 (a) and (b) show the training/validation MSE (loss) and training/validation MAE curves for the MLP-N6 model, respectively. Both the training MSE and MAE values steadily decreased across epochs (see Fig. 2), indicating that the model learned effectively. In addition, the parallel decrease in the training and validation MAE curves confirmed the generalization ability of the model.

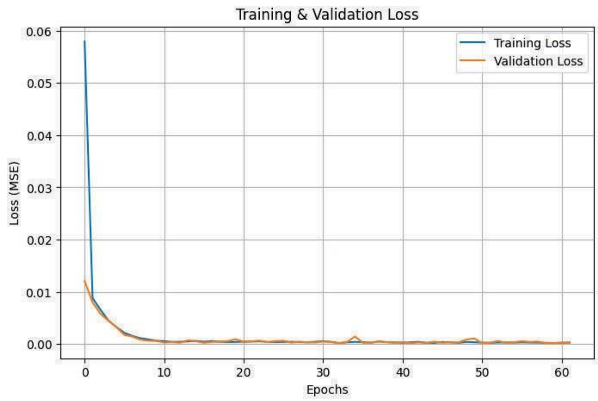

(a)

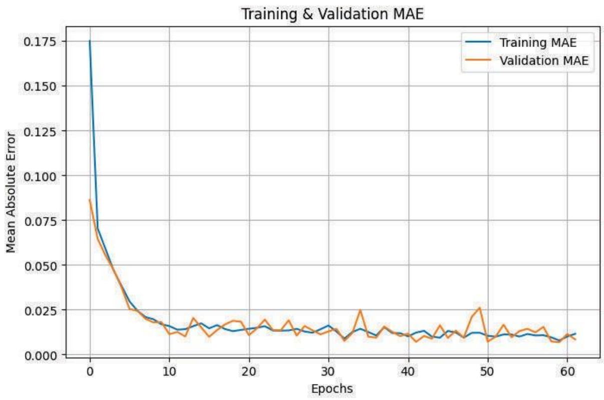

(b)

Fig. 2. Training and validation a) loss and b) MAE curves throughout epochs for MLP-N6

TABLE IV. PERFORMANCE COMPARISON

Ref.	Model	R^2	MSE
This study	MLP-N3	0.9987	0.000190
	MLP-N6	0.9989	0.000164
[12]	Bagging Regressor	0.9985	0.000212
	Random Forest Regressor	0.9984	0.000226

Table IV gives a comparison of the prediction models for the same dataset. Analyzing Table IV, it is concluded that this study achieved better results (the highest R^2 and the lowest error values) than the best results reported in [12].

SHAP analysis was applied to the MLP models to quantify the feature contributions. Fig. 3 illustrates the SHAP summary plot for the trained MLP-N6 model. In the plot, the color gradient, ranging from blue (low) to red (high), indicates the feature values. Frequency had the highest impact on the model predictions, followed by *a* and *h*.

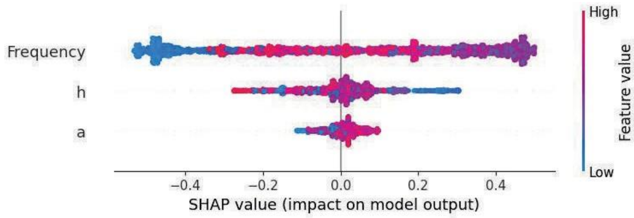

Fig. 3. SHAP summary plot.

Fig. 4 presents the SHAP bar plot for a test sample. This plot visualizes the contribution of each feature to absorbance prediction. A positive SHAP value indicates that the feature improves prediction. All features contributing to the absorption prediction had positive SHAP values, and frequency had the largest positive contribution. By providing transparency in model decision-making, the black box challenge of MLP was addressed.

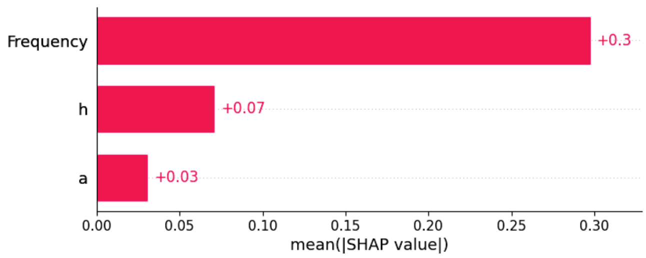

Fig. 4. SHAP bar plot for a sample.

CONCLUSION

In this work, the absorption performance of THz metamaterial absorbers was predicted using a simulation-driven dataset. We investigated an explainable surrogate model that integrates SHAP and MLP. Six different MLP network models were tested, and SHAP technique was leveraged to understand MLP model decisions. Explainability can be used to improve model structure and performance. The contribution of this study lies in the proposed method, which highlights the impact of physical design parameters on absorptance. These findings suggest that the use of explainable frameworks may also be effective in designing other electromagnetic components. This suggests that, during the design process, researchers can benefit from integrating XAI-enhanced machine learning methods to enable rapid evaluation, reduce development time, and ultimately carry out a more efficient workflow.

In future work, the predictive performance of the current surrogate model can be further refined by applying hyperparameter tuning for the MLP architecture, including neurons per layer, activation functions (ReLU, tanh), and optimizers (Adam, SGD), etc. In addition, future studies may focus on the inverse design and various analyses of XAI.

REFERENCES

[1] W. M. Othman, A. A. Ateya, M. E. Nasr, A. Muthanna, M. ElAffendi, A. Koucheryavy, and A. A. Hamdi, "Key enabling technologies for 6G: The role of UAVs, terahertz communication, and intelligent reconfigurable surfaces in shaping the future of wireless networks," *Journal of Sensor and Actuator Networks*, vol. 14, no. 2, p. 30, 2025, doi: 10.3390/jsan14020030

[2] M. S. Akbar, Z. Hussain, M. Ikram, Q. Z. Sheng, and S. C. Mukhopadhyay, "On challenges of sixth-generation (6G) wireless networks: A comprehensive survey of requirements, applications, and security issues," *Journal of Network and Computer Applications*, vol. 233, Art. no. 104040, Jan. 2025, doi: 10.1016/j.jnca.2023.104040

[3] J. Ren, Z. Mu, R. Sellami, *et al.*, "Multifunctions of microwave-absorbing materials and their potential cross-disciplinary applications: A mini-review," *Advanced Composites and Hybrid Materials*, vol. 8, p. 202, 2025, doi: 10.1007/s42114-025-01258-5

[4] J. T. Orasugh, A. Mohanty, A. Malakar, S. Bose, and S. S. Ray, "Design and applications of multi-frequency programmable metamaterials for adaptive stealth," *Advanced Functional Materials*, early access, Aug. 7, 2025, doi: 10.1002/adfm.202513726

[5] N. I. Landy, S. Sajuyigbe, J. J. Mock, D. R. Smith, and W. J. Padilla, "Perfect metamaterial absorber," Physical Review Letters, vol. 100, no. 20, p. 207402, May 2008, doi: 10.1103/PhysRevLett.100.207402

[6] W. Withayachumnankul, K. P. Chen, S. Albani, and D. Abbott, "A review of terahertz metamaterials and metasurfaces: Principles, designs, and applications," Advanced Optical Materials, vol. 7, no. 17, p. 1900162, Sep. 2019, doi: 10.1002/adom.201900162

[7] J. Leng, Y. Gong, L. Luo, and Q. Shi, "Vanadium dioxide-based terahertz metamaterials for non-contact temperature sensor," *Photonics*, vol. 11, no. 12, p. 1148, 2024, doi: 10.3390/photonics11121148

[8] C. Lu, Q. Lu, M. Gao, and Y. Lin, "Dynamic manipulation of THz waves enabled by phase-transition VO2 thin film," *Nanomaterials*, vol. 11, no. 1, p. 114, Jan. 2021, doi: 10.3390/nano11010114

[9] F. Qaderi, T. Rosca, M. Burla, et al., "Millimeter-wave to near-terahertz sensors based on reversible insulator-to-metal transition in VO2," *Communications Materials*, vol. 4, no. 34, 2023. [Online]. Available: https://doi.org/10.1038/s43246-023-00350-x

[10] C. Zhang, Y. Zhang, J. Han, et al., "VO2-based tunable metamaterial absorbers in the terahertz regime," Scientific Reports, vol. 7, no. 1, 2017.

[11] J. Y. Lee, J. H. Kim, H. T. Kim, et al., "Dynamic control of terahertz waves using phase-transition materials," Advanced Functional Materials, vol. 28, no. 10, 2018.

[12] N. Anjum and R. Hasan, "Performance benchmarking of machine learning models for terahertz metamaterial absorber prediction," *arXiv preprint*, arXiv:2508.08611, 2025

[13] P. Mahouti, A. Belen, O. Tari, M. A. Belen, S. Karahan, and S. Koziel, "Data-driven surrogate-assisted optimization of metamaterial-based filtenna using deep learning," *Electronics*, vol. 12, no. 7, p. 1584, 2023, doi: 10.3390/electronics12071584

[14] S. Karasu and S. Ünaldı, "Estimating the Bandwidth of the Metamaterial Antenna with Machine Learning and Feature Importance Methods," in Proc. IEEE International Symposium on Antennas and Propagation and USNC/URSI National Radio Science Meeting, 2023, pp. 1–2.

[15] M. Mersha, K. Lam, J. Wood, A. K. AlShami, and J. Kalita, "Explainable artificial intelligence: A survey of needs, techniques, applications, and future direction," Neurocomputing, vol. 599, pp. 128111, Sep. 2024.

[16] A. Amini, A. Moshiri, M. A. C. Zadeh, *et al.*, "Interpretable artificial intelligence for modulated metasurface antenna design using SHAP and MLP," *Scientific Reports*, vol. 15, Art. no. 24029, 2025. [Online]. Available: https://doi.org/10.1038/s41598-025-10156-1

[17] E. S. Ortigossa, T. Gonçalves, and L. G. Nonato, "Explainable artificial intelligence (XAI)—From theory to methods and applications," *IEEE Access*, vol. 12, pp. 80799–80846, 2024, doi: 10.1109/ACCESS.2024.3409843

[18] N. Anjum, *Metamaterial Absorber Dataset*, Kaggle, 2025. [Online]. Available: https://www.kaggle.com/datasets/nanjum27/metamaterial-absorber-dataset

[19] U. Hasson, S. A. Nastase, A. Goldstein, "Direct Fit to Nature: An Evolutionary Perspective on Biological and Artificial Neural Networks," *Neuron*, vol. 105, no. 3, pp. 416-434, 2020. https://doi.org/10.1016/j.neuron.2019.12.002

[20] W. R. Ashby, "An Introduction to Cybernetics", London, England: Chapman and Hall, 1956.

[21] M. McCloskey, "Networks and theories: the place of connectionism in cognitive science," *Psychological Science,* vol. 2, no. 6, pp. 387-395, 1991. https://doi.org/10.1111/j.1467-9280.1991.tb00173.x

[22] W. Zhang, X. Shen, H. Zhang, Z. Yin, J. Sun, X. Zhang, L. Zou, "Feature importance measure of a multilayer perceptron based on the presingle-connection layer," *Knowledge and Information Systems* vol. 66, pp. 511-533, 2024. https://doi.org/10.1007/s10115-023-01959-7

[23] L. S. Shapley, "A value for n-person games, vol II of Contributions to the theory of games," Princeton University Press, Princeton, 1953.

[24] E. Štrumbelj, I. Kononenko, "Explaining prediction models and individual predictions with feature contributions," *Knowledge and Information Systems,* vol. 41, pp. 647-665, 2014. https://doi.org/10.1007/s10115-013-0679-x

[25] M. Rahimian, L. Iulo, J. P. Duarte, "Chapter 8 - Spatial design of energy self-sufficient communities," *Artificial Intelligence in Urban Planning and Design,* pp. 139-162, 2022. https://doi.org/10.1016/B978-0-12-823941-4.00021-4